

July 9, 2011

StratoSolar Photovoltaic system

Introduction: The goal of this document is to present a short technical introduction while conveying the message that there is a much deeper body of data, analysis, and development effort underlying and supporting this brief summary. There are four main sections: an overview, technical basics, detailed analysis and miscellaneous topics

Overview

What the system does:

- Weather independent, photovoltaic solar power (PV)
- Locations up to latitude 60
- Electricity in utility scale systems from 10 MW to 1 GW in modular increments
- Cost competitive electricity without subsidy

Key insights:

The idea exploits two environmental facts. Firstly, the stratosphere is a permanent inversion layer in the earth's atmosphere. Inversion layers effectively isolate gas bodies. The calm weather free stratosphere is isolated from the turbulent troposphere below. There is no rain, hail, snow, or moisture in the stratosphere and wind force is much reduced and stable. This means that buoyant platforms suspended in the stratosphere can be permanently stationed there without needing to be winched down in bad weather. It also means that PV panels in the stratosphere don't suffer water or snow or ice based weather effects and can be simpler and cheaper to manufacture.

Secondly, light from the sun at 20km altitude is both strong and constant from dawn to dusk. At 20km a platform is above over 90% of the atmosphere, so sunlight is not significantly scattered or absorbed and there are no clouds to interrupt power generation. This means that on average PV panels produce multiples of the power they can generate on the ground, and just as important, the power is highly predictable and not subject to interruption by clouds or storms.

Why it generates electricity at a reasonable cost:

For solar-power plants, almost the complete operating cost is the loan payment. The StratoSolar PV system has a reasonable operating cost mostly because the solar PV array (which dominates PV cost) has a reasonable capital cost and a high utilization, with a resulting reasonable cost of electricity. The reasons for this are:

- The PV panels are exposed to 1.5 to 3.5X the solar energy of ground-based PV panels
- This means each square meter of PV panel gathers 1.5 to 3.5X the energy of ground-based PV panels
- The PV array uses no land. No land cost, or site development cost.

July 9, 2011

- The PV array support structure uses very little material due to light structural loads.
- All construction materials are standard, off the shelf, and low cost
- The PV panels are lower cost than ground-based PV panels due to reduced panel packaging cost

The extra capital costs incurred by the StratoSolar approach are the tether/HV cable, the winch, the gasbags and the hydrogen they contain. Adding everything up the capital cost of a StratoSolar plant in \$/Wp is the same as or lower than the same plant on the ground. However the StratoSolar plant captures substantially more energy and generates substantially more kWh of electricity. Depending on geographic location the overall advantage in the cost of electricity generated in \$/kWh over ground-based PV can exceed 3X. See the detailed analysis section below for more detail on this topic. [Ground PV cost compared to StratoSolar PV:](#)

This is a commercially competitive alternative energy solution. By not covering huge land areas, it saves on an expensive, highly regulated, and uncertain resource that tends to delay construction and limit financing options. It also allows great flexibility in location. The competitive and highly profitable economics should lead to a business that is market financed and does not need government support or subsidy once demonstrated. It is a bonus that this energy is carbon-free, and solves energy security issues.

The idea:

A PV array, permanently positioned in the stratosphere at altitude 10 km to 20 km, gathers sunlight, converts it to electricity and transmits it down a tether/high voltage (HV) cable to the ground where it connects to the electricity distribution grid.

July 9, 2011

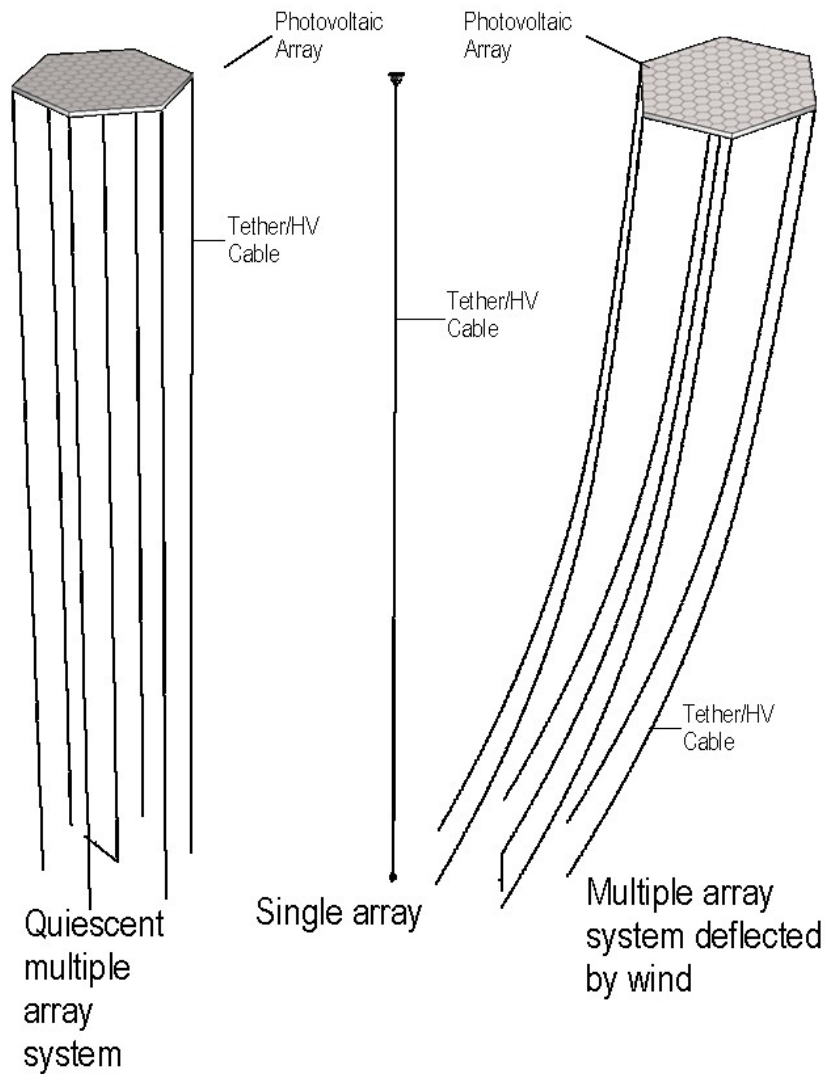


Figure 1

Figure 1 shows an individual PV system in the center. The novel element of a StratoSolar power plant is a buoyant tethered platform supporting an array of PV panels floating in the stratosphere. The strong and light tether incorporates a HV power cable that transfers electric power to the ground. Excess buoyancy in the floating platform pre-tensions the tether and allows the platform to resist wind forces.

July 9, 2011

A rigid truss structure supports the PV array. Buoyancy is from gasbags within the truss framework. Models for the PV array power output are subject to simulation to a high degree of accuracy, with high confidence in the results. While the buoyant structure is novel, there is no new science, and existing engineering design tools are sufficient. The wind and buoyancy forces are well understood from an engineering perspective. There are detailed meteorological models and historical data to provide an accurate statistical profile of the wind and buoyancy forces on the structure and tether. The combination of accurate structural analysis and reliable meteorological data mean that structural viability can be determined to a high confidence level before construction. Accurate models for sunlight and how it varies with location and altitude, daily and seasonally, provide an equally high confidence level for the power output.

Figure 1 also shows two views of a large-scale system, the first view on the left with no wind and the second view on the right with a maximum wind load. The large-scale system is a collection of mechanically connected individual modular small-scale systems. For clarity only some of the tethers are shown. The benefits of connecting multiple smaller systems to make a larger system are reduced aerodynamic drag on the PV array and reduced impact on regulated airspace. The array is directionally stable and panels can track the sun. The reduced aerodynamic drag ensures that the structure can withstand the highest wind forces with a large safety margin and is safe to deploy on a permanent basis. It also facilitates modular maintenance and repair, technology upgrades, and incremental overall system expansion. Individual arrays can be winched down when weather permits and can use adjacent tethers as guides to ensure safe control.

Operationally there should be no need for people at 20km. There is no need for large “hanger” structures, either for construction or maintenance. During construction and maintenance the array structure is anchored at multiple points to the ground and effectively forms a roof over a protected space. Maintenance on the ground only occurs during good weather and at night to avoid disruption in power output. Plants can safely be raised and lowered in a few hours, and with close attention to weather, the window of exposure to unexpected weather is very small.

Another benefit of the modular approach is the system can grow and be financed incrementally, reducing the risk capital required to develop and demonstrate the system viability.

What are the benefits of 20km altitude?

- More sunlight results in lower cost per kWh. Under \$0.10/kWh without subsidy
- Locations as far north as latitude 60 are practical and have the biggest cost advantage
- No land needed for the PV array
- Highly predictable power compared to ground based PV. Weather never affects power.
- No shading effects simplify the electrical design
- The -50°C cold environment at 20km altitude enhances PV efficiency
- At 20km altitude the PV panels don't have to handle rain, moisture, hail, snow or strong wind forces. This reduces their packaging cost significantly

July 9, 2011

- The worst-case wind force on the PV array and the tether is low enough to allow for permanent tethering.

How far removed is it from what has been done before?

The altitude and the scale of the structure required favor a rigid structure rather than a pressurized membrane (blimp) approach which would have difficulty scaling. The largest rigid buoyant structures were rigid airships built in the 1930's and these displaced about 300 tonnes. This was at low altitude of less than 5000 m. However, these show all the basic technologies required in rigid structures and gasbags.

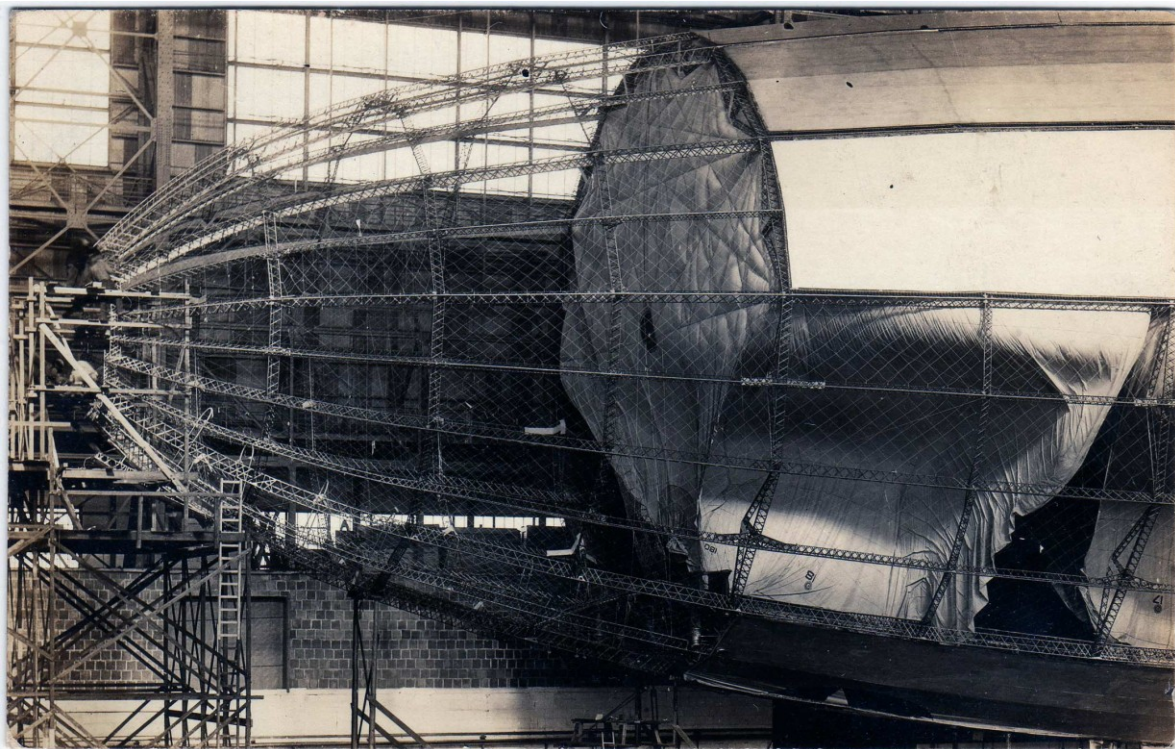


Figure 2

Figure 2 shows the interior structural elements of the Shenandoah. There are rigid triangular aluminum alloy struts, ropes across the struts to contain the gasbag, the partially filled gasbag, and the separate tensioned membrane exterior weatherproof skin all clearly visible. Figure 12 shows the similar internal structural elements of the Hindenburg and the Macon.

A solar PV system would displace about 600 tonnes at 20 km and use the same structural elements but more modern materials. Compared to airships these structures are dramatically simpler. They don't have to comply with an aerodynamic shape; they don't require stability and control surfaces, engines, passenger or crew accommodation etc. Simple trusses made with identical mass produced struts and simple metalized plastic gasbags also mass-produced are sufficient to build the basic structures required.

July 9, 2011

Utility scale systems are a significant jump in scale, but are simply multiple instances of the smaller modular system. The benefits of connecting multiple smaller systems to make a larger system are reduced drag on the PV array structure and reduced impact on regulated airspace. The multiple tethers make the system directionally stable and benefit from sun tracking.

The highest tethered aerostats have been at about 8 km ⁽¹⁾ [TCOM](#) (Figure 13), though science projects have proposed and investigated aerostats at 12 km and higher ⁽²⁾. While smaller in scale, these aerostats demonstrate the technology for lightweight tethers (and their associated winches) that integrate power transmission and communications and handle lightning. Most research balloons that have flown in the stratosphere have been untethered.

For this concept to become commercially viable what are the real problems and what technologies are available to solve them?

The biggest issue is tethering a large structure at 20km. This has never been done before and raises considerable skepticism. This skepticism seems to be primarily psychological as the technology required is very basic. To overcome this skepticism we propose to proceed incrementally by first developing a smaller tethered test platform that will float at 20km altitude. This will be an approximately one third to one half scale version of a 10MW platform using the same construction materials and techniques. This will demonstrate the feasibility of the technology and allow for testing the design elements in the stratosphere, particularly the lightweight PV panels. The test platform will use a simple tether that does not transmit power and will only carry a few prototype lightweight PV panels. The test platform and associated tether and winch will cost less than \$500,000. Figure 3 shows the relative scale of the test platform to a 10MW platform. As shown the construction is identical. The test platform has 30m to 50m struts, and the 10MW platform has 90m to 110m struts. In both cases there are 102 primary struts.

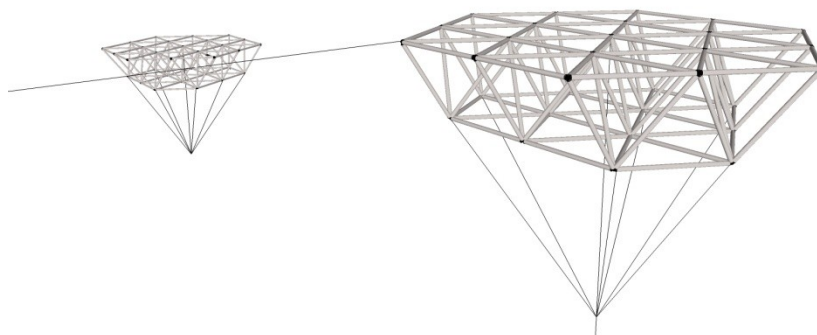


Figure 3

July 9, 2011

The risk factors are the same risks faced in all large-scale structures. The balance of importance may be different but fire, lightning, ice, weathering, wind, etc. are always issues faced (and solved) by all large-scale structures.

The PV array does not face water-based weathering or dust and dirt, but does face increased UV, ozone and -50°C cold. Lightning up strokes that affect the PV array are possible. Depending on altitude the tether faces a variety of weather effects including rain, hail, icing and lightning strikes.

The two larger questions are about big environmental inputs, the sun and the wind. How much light is there at 20 km and how does it vary by location, time of year, and time of day? What are the dispersion and wavelength characteristics? How much wind is there through the 20 km vertical profile, and how does it vary statistically by time and location?

At this stage, we have lots of data and accurate models for both wind and sunlight. These provide high confidence that the structural and power designs are practical.

The StratoSolar concept is now at an early evaluation stage. It's clear that it is physically possible. The questions revolve around the practicality. It will take building a prototype to address the myriad concerns about the practicality. StratoSolar is an evolution of current ground based PV systems. It is feasible based on detailed simulation. It needs to pass the practicality hurdle. Our plan is to do this incrementally and at low cost.

The first step is a 12-month R&D effort that will develop the design of a modular 10MW system and accurately simulate its mechanical and electrical behavior. The R&D phase will also develop and deploy a tethered test platform that will fly at 20km and allow testing of lightweight PV panels, gasbags and structural elements.

The second step is to construct a power generating 10MW system using the elements designed, developed and tested during step one.

July 9, 2011

Technical Basics:

PV array structure:

The PV array structure shown in Figure 4 is a simple tetrahedral truss framework containing large gasbags that provide buoyancy. A few simple calculations using the Archimedes principle show that supporting the PV array with a buoyant structure violates no laws of physics or practicality. Let us model the collector as a disk 350 m in diameter and 94 m thick with the volume filled with hydrogen gasbags. The volume is then approx. $9.0e6 \text{ m}^3$. The density of air at 20 km is about one tenth that at sea level and 1 m^3 filled with hydrogen can lift about 0.1 kg. The disk structure can then lift about $9.0e5 \text{ kg}$, or 900 tonnes.

Buoyancy becomes more effective for large structures because the volume to surface area ratio increases. This along with the air density sets the practical limit for minimum size structures for the payloads desired and the structural materials that are practical. For this system the payload is the PV panels and the tether.

Being a buoyant structure with the buoyancy evenly distributed throughout, the structure does not have to sustain its own weight.

This is a substantial benefit. Over half of the force (and hence half the structural strength requirement) on regular structures is due to gravity. The structure is tethered, however, and so will have to sustain wind forces.

The wind forces in the stratosphere are always light and steady and a fraction of the worst-case ground wind force. The combination of buoyancy effectively canceling gravity and much lighter wind loads results in a practical lightweight structure.

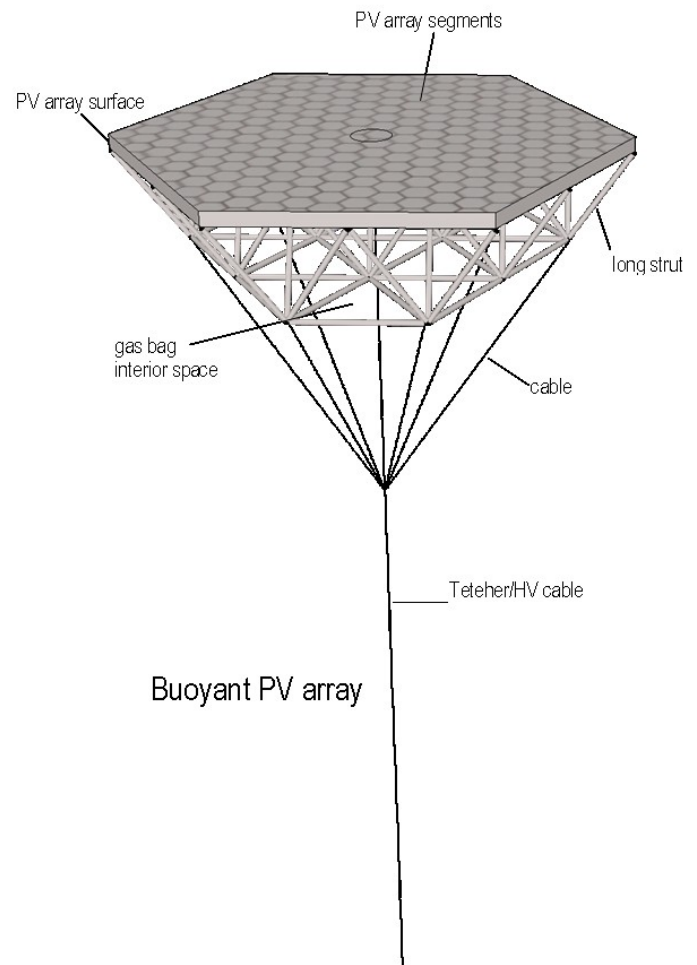


Figure 4

July 9, 2011

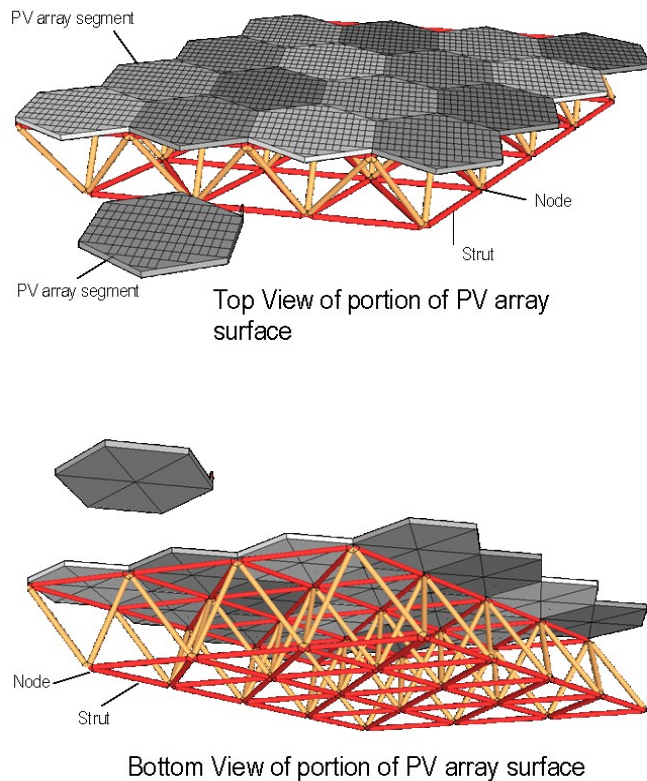


Figure 5

protection from weather or the sun. Metalized plastic films can hold unpressurized hydrogen losing only a fraction of a percent a year. A small-diameter hose from the ground attached to the tether can supply hydrogen to replace leakage. Lightweight cords strung across the struts confine gasbags and transmit the buoyancy force to the rigid truss structure. This was the method employed by rigid airships. This allows the gasbags to conform to the truss as they expand from their initial partially filled state. The ozone concentration at 20 km (2.8 ppm) requires care in the choice of plastic material and/or methods to protect it.

The hexagonal lightweight PV array elements attach to the rigid structural frame as shown. The PV panels use identical PV cells and supporting electrical elements as those already in use on the ground. It is relatively easy to adapt to PV cells of different technology or from different vendors.

Many truss designs are possible. All minimize the number of unique elements for ease of production and assembly. Struts are similar in construction to those used in rigid airships and use triangular truss aluminum alloy construction for low cost. The reference design shown employs a tetrahedral aluminum alloy truss. Figure 5 shows a top view and a bottom view of a small section of the top surface truss supporting hexagonal PV array elements. The struts shown are about 17 m long. The hexagonal PV array elements have 10 m sides and hold about 100, 2m² PV panels. Larger struts (not shown), also forming a tetrahedral truss, form the 94 m depth of the PV array structure that holds the gasbags.

Unlike blimps, gasbags in rigid structures only have to contain gas. They don't have to provide structural strength or provide

More detailed analysis topics

Wind Force:

In the prior art, tethered aerostats and balloons have been winched down when subject to excessive wind forces. The goal for StratoSolar systems is to remain aloft through worst-case wind loads, and so it is important to understand what those worst-case wind loads are. There are two distinct wind environments; the troposphere where the winds act on the tether/HV cable, and the stratosphere where the winds act on the PV array structure. This section discusses the sources of the wind data and establishes the maximum wind forces used in the design of the tether and array. A later section describes the design and simulation of the tether and array that handles these wind loads.

Wind force is dependent on location and varies seasonally. The Integrated Global Radiosonde Archive (IGRA)^{(10) (11)} is a substantial and important meteorological database that contains wind speed and atmospheric pressure data for 50 years or more for over 2000 sites worldwide. Weather prediction was the original object of this data collection. The data is a highly reliable and public record exceeding 10 GB. It provides wind speed and air density data directly, but not wind force, which is what we are most interested in. Wind force depends on the product of air density and wind velocity squared. We have used the IGRA data to calculate average wind force over a 20 km vertical profile in order to establish accurate statistical confidence levels for wind force in the troposphere and the low stratosphere. This is a critical input to the design of the tether and the PV array structure. From analyzing the data, it is clear that wind force is very site specific. The 95% utilization averaged wind force varies from 28 Pa to 481 Pa from the lowest wind site to the highest wind site, with a linear distribution for sites between both extremes. It is also apparent that the optimal height for the PV array structure is site dependant, and lowers with increasing latitude. It appears that optimal placement is slightly above the tropopause. 20 km works well for northern California.

Table 1 shows an example of the analyzed wind force data for the Oakland, California site. The column marked “#” shows the number of valid records used for the corresponding row statistics. All other columns are wind pressure in Pa. The “%” columns represent the average pressure exceeded by that percentage of samples. For example from the “ALL” row the average of the highest 5% of the wind pressures is 239.8 Pa. The maximum average wind force recorded for Oakland is 525.9 Pa and occurred in December 1971. The design assumption is that the power plants will remain operational under extreme weather conditions. This worst-case pressure sets the wind design criterion for the tether.

The monthly data shows seasonal variability and the yearly data shows long-term variability.

Based on this statistical data we can generate a vertical wind profile for the desired site and use that in the design of the tether and PV array structure.

Station name: OAKLAND US

Station location: lat 37.75, long -122.22 station geometric elevation: 6 m

0-20 km average wind force

StratoSolar PV system

July 9, 2011

Table 1 Tether wind force

when	#	avg	std	min	10.00%	5.00%	2.00%	1.00%	0.50%	max
Jan	581	96.87	67.08	1.5	234.8	261.5	294.9	327.9	367.2	401.6
Feb	577	91.2	64.95	5.2	230	254.9	278.6	293.2	302.7	323.1
Mar	577	85.48	59.73	1.2	211.2	240.5	275.1	301.4	326.2	379.2
Apr	568	91.54	64.9	2	229.9	256.1	285.3	298.9	309.8	324.2
May	584	76.43	59.97	1.5	207	237.6	269.2	296	326.8	336.8
Jun	539	58.68	45.15	0.2	153.8	178.2	207.9	238	264.5	304.6
Jul	585	38.64	32.68	0.6	111.6	133.9	157.3	173.1	183	185.2
Aug	564	42.74	32.74	1	117.3	135.9	153.6	160.5	171.2	182.6
Sep	538	49.16	41.08	1	137.5	154.1	174.3	185.6	186.6	189.6
Oct	564	66.21	56.79	0.7	194.3	227.7	276.3	303.4	327.3	343.3
Nov	577	100.58	65.15	3.5	236.2	267.4	304.4	335.8	366.1	400.2
Dec	597	90.81	69.57	4	239	280	344.3	404.6	466	525.9
1970	100	104.07	89.28	5.4	302.4	355.9	391.6	400.2	400.2	400.2
1971	24	162.38	130.16	10.7	463.8	525.9	N/A	N/A	N/A	525.9
1972	27	107.05	72.31	13.9	228.8	234.6	234.6	N/A	N/A	234.6
1973	29	128.82	73.18	9.5	271.6	289.1	289.1	N/A	N/A	289.1
1974	7	92.96	106.51	14.2	264.7	N/A	N/A	N/A	N/A	264.7
1975	30	133.98	79.48	12.6	287.8	319.2	355	N/A	N/A	355
1976	78	82.92	62.69	6.2	219.7	233.3	241.8	248.6	N/A	248.6
1977	52	103.59	86.24	6.6	307	332	379.2	379.2	N/A	379.2
1978	33	108.96	110.21	9	376.1	413.8	489.1	N/A	N/A	489.1
1979	27	104.88	79.99	4.7	245.3	275.5	275.5	N/A	N/A	275.5
1980	35	89.77	55.17	1.5	199.4	227.8	236.7	N/A	N/A	236.7
1981	8	106.09	52.74	20	181.9	N/A	N/A	N/A	N/A	181.9
1982	9	88.37	69.45	4.6	199.5	N/A	N/A	N/A	N/A	199.5
1983	4	107.83	37.07	52.5	N/A	N/A	N/A	N/A	N/A	130.3
1984	11	65.45	45.37	17.6	178.2	178.2	N/A	N/A	N/A	178.2
1985	32	62.86	64.69	6.6	215.6	242.8	300.1	N/A	N/A	300.1
1986	35	69.62	63.65	0.2	185.8	201.2	226.3	N/A	N/A	226.3
1987	90	74.7	66.6	2.6	210.2	228.3	239.3	246.2	N/A	246.2
1988	97	81.06	67.34	2.3	230.1	267.9	304.2	309	N/A	309
1989	63	89.84	56.5	5.7	203.1	228.4	242	242	N/A	242

July 9, 2011

1990	509	77	59.96	2	206.9	243	278.9	299.7	314.8	343
1991	509	68.31	61.54	1	208.8	241.6	268.6	282.8	290.7	305.1
1992	425	61.57	50.23	1	172.2	192.6	214	232.6	238.7	240.6
1993	430	73.9	51.07	0.7	178.4	199.9	236	263	277.7	282.4
1994	471	71.08	53.58	1.2	187.2	215.3	260.9	281.3	314.4	342.6
1995	497	71.26	55.53	2.4	192.6	221.4	248	263.7	267.8	268.3
1996	497	76.64	62.21	0.8	215.1	243.4	277.9	304.4	335.7	336.8
1997	513	76.9	63.36	0.6	216	244.8	280.7	298.3	308.3	324.2
1998	557	78.94	61.54	1.2	211.1	242.3	272	285.9	302.9	326.9
1999	512	67.32	55.64	1.3	191.6	213.6	240.5	256.7	267.2	304.7
2000	540	68.67	54.7	0.9	191.1	215.6	239.7	258.4	268.7	286.2
2001	600	68.1	52.67	0.3	185.6	214.1	250.2	278.6	315.5	393.8
ALL	6851	74.33	60.45	0.2	207.4	239.8	278.2	307.2	339.6	525.9

Table 2 shows the IGRA-derived wind force for 20 km altitude, which determines the force on the PV array structure. There are more years covered for this table because more samples met the simpler criteria. From the "ALL" row the wind force that is exceeded 5% of the time is 23.4 Pa. The criteria for wind samples for 20 km include the nearest sample within 2 km of 20km. This results in the acceptance of some samples as low as 18 km. These samples account for the exceptional high wind forces in the max column, and highlight the necessity to design the PV array structure to handle the occasional exceptional high-altitude troposphere wind. For example the exceptional wind force on one occasion in September 1985 was for a sample near 18km.

Oakland 20 km wind force.

Table 2 PV array stratospheric wind force

when	#	avg	std	min	5.00%	2.00%	1.00%	0.50%	0.20%	0.10%	max
Jan	2918	3.66	5.54	0	21.3	30.1	38.5	49.2	69.5	89.3	96.3
Feb	2767	3	5.2	0	18.3	25.9	33.6	43.3	61.1	87.5	165.9
Mar	3026	2.94	4.87	0	18.8	28	35.9	44.1	60.2	74.1	86.5
Apr	2967	2.29	4.09	0	15.3	24.5	32.5	40.1	48.6	55.6	73.3
May	3091	0.99	2.51	0	6.8	11.4	17.1	26.4	45.8	58.2	85.1
Jun	3067	1.24	2.78	0	5.8	8.7	12.3	19.1	36.5	63.3	135.3
Jul	3251	2.13	1.57	0	6.1	7.3	8.4	10	12.9	18.3	33.2
Aug	3125	1.53	1.81	0	5.5	7.4	9.5	12.4	20.9	32.8	73.8
Sep	3031	1.08	8.17	0	7.8	14.2	23.6	41.2	90.4	166.1	390.8
Oct	3098	1.89	3.26	0	9.9	14.1	18.8	26.3	42.1	61.9	130.9
Nov	2777	3.28	4.95	0	17.4	24.8	32.2	42.3	60.4	87.6	140.8
Dec	2883	3.91	21.21	0	27.4	46.8	72.3	118	224.6	404	404

StratoSolar PV system

July 9, 2011

1948	44	2.11	2.58	0	10.5	13.3	N/A	N/A	N/A	N/A	13.3
1949	33	2	2.01	0	8.4	8.9	N/A	N/A	N/A	N/A	8.9
1950	12	2.67	2.04	0	5.9	N/A	N/A	N/A	N/A	N/A	5.9
1951	7	1.93	1.09	1	N/A	N/A	N/A	N/A	N/A	N/A	4
1952	12	2.09	2.11	0	5.7	N/A	N/A	N/A	N/A	N/A	5.7
1953	12	2.74	2.17	0.2	6.7	N/A	N/A	N/A	N/A	N/A	6.7
1954	101	2.17	2.44	0	10	11.8	13.1	13.1	N/A	N/A	13.1
1955	763	2.79	3.84	0	15.3	22.3	28.1	33.9	39.4	42.3	42.3
1956	733	2.02	2.22	0	8.8	10.7	12.1	13.3	20	20	20
1957	721	2.67	4.23	0	17.1	25.7	33.2	37.5	51.6	51.6	51.6
1958	545	1.48	1.64	0	6.8	9	10.6	11.3	13.1	13.1	13.1
1959	630	1.87	2.27	0	8.9	11.9	14.7	16.6	18.3	18.3	18.3
1960	611	2.13	2.35	0	9.8	12.5	14	15	16.4	16.4	16.4
1961	661	2.49	3.95	0	16.2	23.8	29	36	44.8	44.8	44.8
1962	672	2.11	2.71	0	11.2	14.3	15.9	19	22.9	22.9	22.9
1963	662	3.67	5.88	0	24.5	32.3	36.8	45.1	51.7	51.7	51.7
1964	667	1.96	2.93	0	12.3	17.2	19.5	22.2	24.3	24.3	24.3
1965	679	2.16	3.88	0	15.3	24.9	30	31.8	33	33	33
1966	666	2.39	4.34	0	15.2	23.5	31	46.7	75.3	75.3	75.3
1967	684	1.97	3.01	0	11.3	16.3	22.1	32.2	38.4	38.4	38.4
1968	685	2.7	17.52	0	27.2	55.2	98.3	189.9	189.9	189.9	189.9
1969	688	2.63	5.18	0	19.9	27.8	35.8	50.9	86.5	86.5	86.5
1970	688	2.15	2.42	0	9.6	12.5	15.2	18.5	22	22	22
1971	609	2.51	4.67	0	17	27.4	36.9	47.3	73.3	73.3	73.3
1972	605	2	2.36	0	9.4	13.4	16.8	18.6	21.3	21.3	21.3
1973	522	1.96	6.56	0	14.8	27.9	44.4	63	140.8	140.8	140.8
1974	442	1.77	2.37	0	10.1	13.2	16.1	20.2	21.6	N/A	21.6
1975	633	1.89	2.83	0	11	15.9	21.7	27.3	36.5	36.5	36.5
1976	692	1.45	1.79	0	6.9	9.8	13.4	18.1	23.4	23.4	23.4
1977	666	1.69	2.13	0	8.4	11.5	14.1	18.2	21.9	21.9	21.9
1978	662	2.38	4.74	0	18.7	28.7	35.9	46.9	50.9	50.9	50.9
1979	663	1.79	2.1	0	8.6	10.7	11.6	12.8	14.9	14.9	14.9
1980	660	2.09	3.78	0	15.2	22.3	28.4	35.6	43.3	43.3	43.3
1981	650	2	2.85	0	11	16.2	19.9	25.9	32.5	32.5	32.5
1982	593	1.79	2.34	0	9.2	11.8	14.1	17.4	24	24	24
1983	565	1.85	3.02	0	11.4	18.2	24.3	31	32.8	32.8	32.8
1984	629	2.33	4.13	0	14.7	23.7	34.7	46.8	58.5	58.5	58.5
1985	618	4.55	44.8	0	53.1	114.1	208.8	390.8	390.8	390.8	390.8
1986	565	1.7	2.37	0	9.7	13.7	16.2	19.1	23.1	23.1	23.1
1987	644	1.84	5.14	0	13.6	24.7	42	68.4	85.1	85.1	85.1
1988	595	2.13	3.17	0	13.2	17.4	20.1	22.5	24.3	24.3	24.3

July 9, 2011

1989	528	1.93	2.37	0	9.8	12.6	14.5	15.7	18.7	18.7	18.7
1990	701	2.68	3.99	0	16	24.5	30	34	40.7	40.7	40.7
1991	692	2.75	4.8	0	19.9	28	35	43.8	49.4	49.4	49.4
1992	625	2.84	7.12	0	26.3	40.9	57.7	77.5	96.3	96.3	96.3
1993	621	1.93	2.22	0	8.8	10.4	11.4	12.4	13.6	13.6	13.6
1994	617	2.44	3.31	0	13.4	17.8	21	21.9	22.6	22.6	22.6
1995	669	2.07	3.01	0	10.7	15.7	20.8	32.1	47.6	47.6	47.6
1996	660	2.78	6	0	16.8	26.5	37.7	65.1	130.9	130.9	130.9
1997	683	2.06	2.91	0	12.2	16.4	18.2	20.8	25.9	25.9	25.9
1998	667	3.26	3.93	0	16.6	22.1	25	27.8	29.1	29.1	29.1
1999	673	2.35	5.86	0	14.5	25.7	38.3	65.4	135.3	135.3	135.3
2000	671	2.09	3.08	0	12.3	18.7	22.9	27.9	31.4	31.4	31.4
2001	748	2.1	2.74	0	11.3	15.1	18.8	21.1	23.8	23.8	23.8
2002	632	2.58	7.35	0	17.2	30.2	52	83.1	165.9	165.9	165.9
2003	672	1.88	2.43	0	9.3	12.8	15.7	21.4	33.7	33.7	33.7
2004	612	1.99	2.83	0	11	15.6	20.1	26.3	36.3	36.3	36.3
2005	626	1.9	2.7	0	11.2	15.2	18.6	22.5	29	29	29
2006	720	3.43	5.22	0	19.3	26.8	34.4	42.3	75.1	75.1	75.1
2007	699	1.47	2.42	0	8.7	13.7	19	26.8	35.4	35.4	35.4
2008	680	2.59	5.29	0	21.5	33	39.7	48.9	60.3	60.3	60.3
2009	672	3.64	4.74	0	19	27.2	33	36	40.8	40.8	40.8
2010	144	2.34	2.87	0	12	14.8	18.2	18.2	N/A	N/A	18.2
ALL	36001	2.3	7.42	0	14.9	23.4	32.6	45.4	72	107.5	390.8

High altitude airship wind force:

In recent years interest in high altitude airships (HAA) for surveillance and communication has led to investigation of winds at 20km altitude. Work based on the NCAR/NCEP reanalysis data which includes satellite Doppler wind measurements going back to 1979⁽¹²⁾ is consistent with the IGRA data analysis and provides insight into the sources of stratospheric wind variability. In the analysis cited above, winds at 20km altitude never exceed 50 ms, and match the IGRA statistical profile. Again the expectation is that the PV array structure operates in the highest winds.

July 9, 2011

Sunlight intensity:

Sunlight intensity at ground level is well studied and documented for most geographical areas of interest. PV panels operate on both direct sunlight and scattered diffuse sunlight, and the available data measures the total of the two.

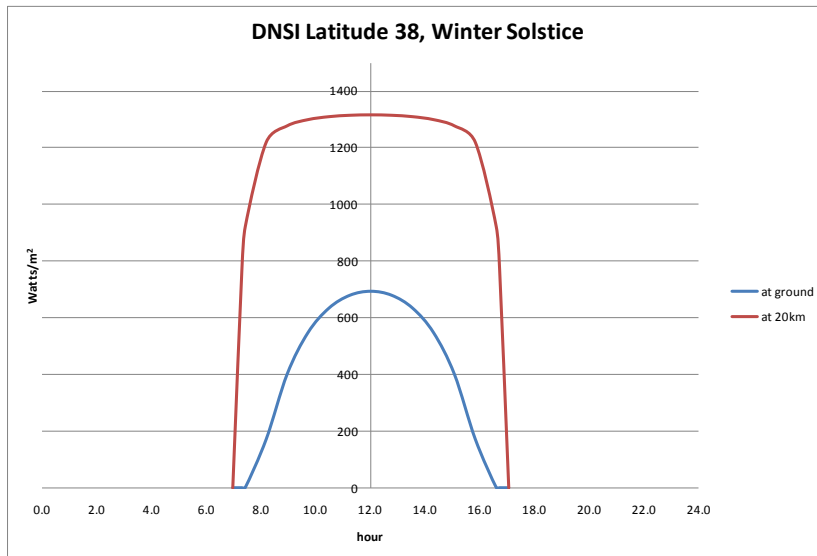


Figure 6

No comparable data exists for sunlight at high altitude in the atmosphere, but sunlight and its interactions with the atmosphere are well understood, and accurate models exist that can predict absorption and scattering through the atmosphere (e.g. MODTRAN). It is easy to use such models to compute DNSI at 20km altitude, though models for the scattered sunlight

component are not as reliable.

At 20km this scattered light is a

small additional energy input we ignore. We have adapted a simplified model from Young⁽¹³⁾ that, given azimuth angle, calculates relative air mass accounting for diffraction. We calculate azimuth angle given the latitude, the day and the hour. Then we calculate relative air mass for ground level and 20 km altitude. This then allows us to calculate direct sunlight in Watts/m² for 20km. The target location for the first StratoSolar prototype system is northern California, so we use Latitude 38 as a relevant example. Figure 6 is a graph of light intensity for latitude 38 on the winter solstice. The horizontal axis is hour, with noon at 12.0. The vertical axis is direct normal solar insolation (DNSI) in Watts/m². The red line is sunlight through the day at 20 km. The blue line is sunlight at the ground with clear skies. Integrating the areas under the curves gives daily Wh/m² of incident solar energy. For this winter solstice case at 20 km, this is 11,800 Wh/m². For the summer solstice, the number is 18,880 Wh/m². The daily average over a year is 15,400 Wh/m².

At higher latitudes, the difference between summer and winter is much more pronounced, and the difference between energy at 20 km and the ground is even more pronounced. For latitude 60, the numbers for 20km altitude are 6,300 Wh/m² at winter solstice and 22,300 Wh/m² at summer solstice. The daily average is 14,300 Wh/m² which is only a 7% reduction from the latitude 38 daily average.

July 9, 2011

Latitude	Location	ground kWh/day	Utilization	20km kWh/day	Util	20km 2-axis kWh/day	Util
34.8	Barstow	5.77	24%	8.55	36%	16.38	68%
	San Francisco	4.76	20%	7.70	32%	15.74	66%
34.7	Osaka	4.00	17%				
42.3	Boston	3.86	16%				
41.8	Chicago	3.62	15%	7.37	31%	15.10	63%
46.8	Quebec	3.61	15%				
47.6	Seattle	3.23	13%				
48.7	Stuttgart	3.06	13%	6.85	29%	15.01	63%
53.5	Hamburg	2.67	11%				
59.3	Stockholm	2.64	11%	6.00	25%	14.30	60%
51.5	London	2.66	11%				
53.3	Dublin	2.30	10%				

Table 3 Average daily solar energy kWh/m² and associated utilization factor for selected locations

The ground columns in Table 3 show average daily kW.h per square meter of total sunlight for selected locations. This is real data gathered over many years by [NREL](#) and others. The data shown is for flat plate horizontal collectors. The 20km columns show StratoSolar data for the selected latitudes generated using the models described above. Simple StratoSolar systems will be horizontal flat plate. Varying degrees of tracking are possible, and real systems will have results intermediate between flat plate and 2-axis tracking. StratoSolar data points illustrate that the average daily kW.h diminishes slowly with increasing latitude at 20km altitude. This means that the power output from a StratoSolar PV system is fairly independent of geography, unlike ground based PV systems which as the table shows gather less energy per square meter at higher latitudes and are therefore significantly less cost effective. For example a simple flat plate StratoSolar system at latitude 60 has a higher utilization than the best surface system in the desert. For daily average kWh/m² data (the most common available), the PV utilization factor is simply the kWh/m²/day divided by 24.

Systems under wind load:

The graphs in Figure 7 below show the results of simulations of a single module/tether (top four graphs) and a 100 module PV array system (bottom two graphs) with multiple tethers subjected to average and maximum wind loads in the troposphere and the stratosphere. The vertical axis is altitude in kilometers. The horizontal axis is down-wind deflection in kilometers. The module design assumes the following parameters. The PV array radius is 175 m and depth is 94 m. The radius of the tether is 0.04 m. The large array is 100 of the modules mechanically joined to form a thin disk 3500m in diameter and 94m deep.

The 2D calculation models the tethers as 20 rigid segments connected by pin joints. The calculation is iterative. The wind force on each segment is calculated and depends on the angle of the tether and the

July 9, 2011

altitude. It also depends on the coefficient of drag, wind velocity and air density. Weight for each segment is also calculated. The length of each tether segment lengthens to maintain the platform at 20km altitude and model the tethers “playing out” under wind load. The wind force for each segment changes with altitude and updates iteratively. The desired maximum deflection sets the required amount of buoyancy.

The top four graphs show progressively stronger wind loads. The sequence from left to right is

- 1) average winds in the troposphere and the stratosphere
- 2) maximum winds in the troposphere, average wind in the stratosphere
- 3) average winds in the troposphere, maximum winds in the stratosphere
- 4) maximum winds in the troposphere, maximum winds in the stratosphere

Average winds are from NASA charts. Worst-case troposphere winds are from NASA and IGRA. Worst-case stratospheric wind is from HAA research. The graphs show relatively small deflections due to troposphere winds exceeding hurricanes acting on the tethers. The winds in the stratosphere acting on the buoyant platform have the most influence on the maximum deflection of the platform.

The goal of the simulation is to verify the practicality and the cost of the solution. The quantities of two materials dominate the wind related costs; the polymer tether cables and hydrogen gas used for buoyancy. For this simulation, 62 tonnes of polymer cables are required at \$20/kg for a total of \$1,245,165. The hydrogen required is 53 tonnes at \$6/kg for a total of \$319,000.

The bottom two graphs in Figure 7 show winds acting on the large array. Two cases are shown, maximum troposphere with average stratosphere, and maximum troposphere with maximum stratosphere. These show the aerodynamic scaling benefit of the large array. Deflection is much smaller under worst-case stratospheric wind.

July 9, 2011

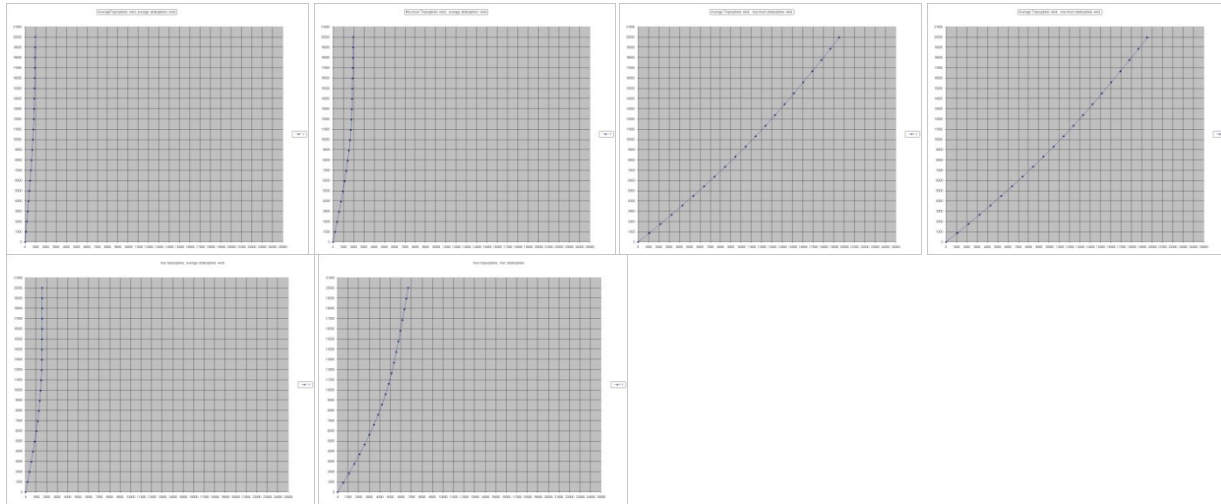


Figure 7 Tether and PV array deflection under wind loads

Accurate models for the aerodynamic behaviors of cylinders also allow the calculation of vortex-shedding induced forces ⁽¹⁶⁾ on the tether. These are high frequency and low amplitude. Asymmetric aerodynamics of a structure cause the more dangerous “galloping” forces. For example, asymmetric ice buildup causes galloping in the case of power cables.

This is a simple static model. It is possible, using engineering software tools, to simulate the system with an accurate meteorological wind model that then drives a simulation of the aerodynamic and dynamic behavior of the structure. This is one of the goals of the funded R&D stage. Accurate computer simulation can test and verify much of the risky engineering.

The current simulations show that for a 10MW system the tether/HV cable is a significant cost element. As systems scale, the tether cost scales with the square root of the size of the PV array and is a proportionately smaller cost.

July 9, 2011

Issues of concern:

There are significant challenges, as with any new large-scale engineering venture. Listed below are some concerns that have been raised. The underlying deep concern is the possibility of catastrophic events that might destroy a power plant and/or expose people to harm. All power plants have such potential catastrophic events, but this concept seems intuitively more exposed than most and until the possible catastrophic events are deemed manageable or at least very unlikely, buoyant stratospheric platforms are not likely to be regarded as a viable option, despite their advantages.

The two most likely sources of catastrophic loss are extreme weather and fire. The modular PV array provides many layers of redundancy, and is designed to handle beyond known worst-case winds and stay operational. The possibility of fire either induced by electrical failure, lightning or static electricity is real, and the ability of the structure to limit the probability of fire, and then to both passively and actively limit fire damage is crucial to the perceived viability.

Here is a list of some concerns.

- The stratosphere is a harsh environment. UV, ozone, and cold are worse than at the ground
- Ice can form on the tether. This could cause a falling-ice hazard or damage the tether through excessive loading
- Wind damage could cause flying debris ripped from the PV array
- The tether or the PV array could fall down causing severe damage on the ground
- The systems might interact with the earth's atmospheric static charge, discharging it
- Lightning, static electricity
- Fire
- The PV panel surfaces may accumulate dust reducing optical efficiency by an excessive amount
- Planes can collide with the tether, and possibly the PV panel array
- Terrorists or vandals could easily damage the tether
- Wind forces on the tether and/or the PV panel array will cause excessive motion through "galloping" resonance effects
- Wind forces are too large for the system to handle
- FAA and/or other regulatory agencies could block or delay construction
- The array will cast a large shadow

Beyond electricity generation:

A permanent high altitude platform could serve many additional purposes. Listed below are some examples of possible uses.

- Communications and observation platform
 - Cell phone tower, data networks
 - Radar for weather, commercial, military
 - Science: astronomy, meteorology, earth science
 - Laser communications network

July 9, 2011

- Tourism

July 9, 2011

Ground PV cost compared to StratoSolar PV:

As shown earlier in the [Sunlight intensity](#) section, a solar PV array at 20 km altitude gathers 1.5 to 3X more energy per m² than a ground-based system. An alternative perspective is StratoSolar needs one-half to one third of ground based PV array area to generate the same electricity. PV array surface area directly determines PV array cost. In addition ground based PV needs land for the array. Figure 8 below graphically illustrates the relative areas for StratoSolar PV panels and ground based PV panels and land.

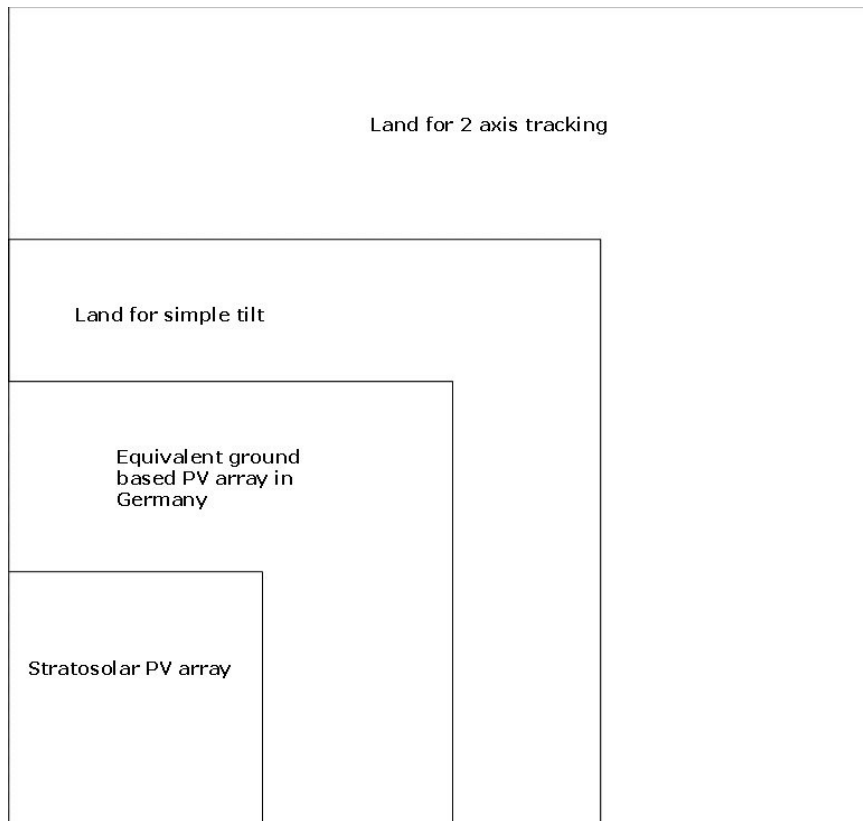


Figure 8 PV array area comparisons

Additional PV array costs for ground-based PV are the land cost and the construction cost to prepare the site and install the PV array. The land area required for a 1 GW peak PV system is about 10 km² (3.8 square miles) assuming flat 10% efficient PV panels and a flat site. Static tilted panels reduce the panels needed by 10% to 15% but double the land required to 20 km². Two axis tracking panels reduce the panel area by about 35% but need five times the land (50 km²). This land and its associated development cost is a significant additional expense. In Germany and other European countries, Japan and the northeastern United States flat clear land is a scarce and expensive commodity. Regulatory approval is a long drawn out political processes that introduce significant risk and can significantly delay or cancel projects.

July 9, 2011

Published estimates for the cost of electricity from current PV plants are \$0.75/kWh to \$0.25/kWh. StratoSolar PV array electricity cost estimates are for \$0.08/kWh initially and less than \$0.04/kWh as PV technology improves.

A 1 GWp PV system in Germany produces from 900GW.h to 1250GW.h per year depending on location. A conventional 1GW coal or nuclear power plant provides about 8,000GW.h per year, so it takes from about 5GWp to 10GWp PV on the ground to match a 1GW utility scale power plant.

There is growing environmental concern concerning utility scale PV plants. They have to keep the ground clean and clear of vegetation, which destroys the local habitat. They consume large volumes of water to regularly clean the PV panels, which is a big problem in desert locations. They also are far from population centers and existing transmission infrastructure, which requires expenditure of billions of dollars on new transmission lines. They require backup gas turbine generators to handle intermittent outages from bad weather. The real cost of utility scale PV plants rarely includes these additional costs.

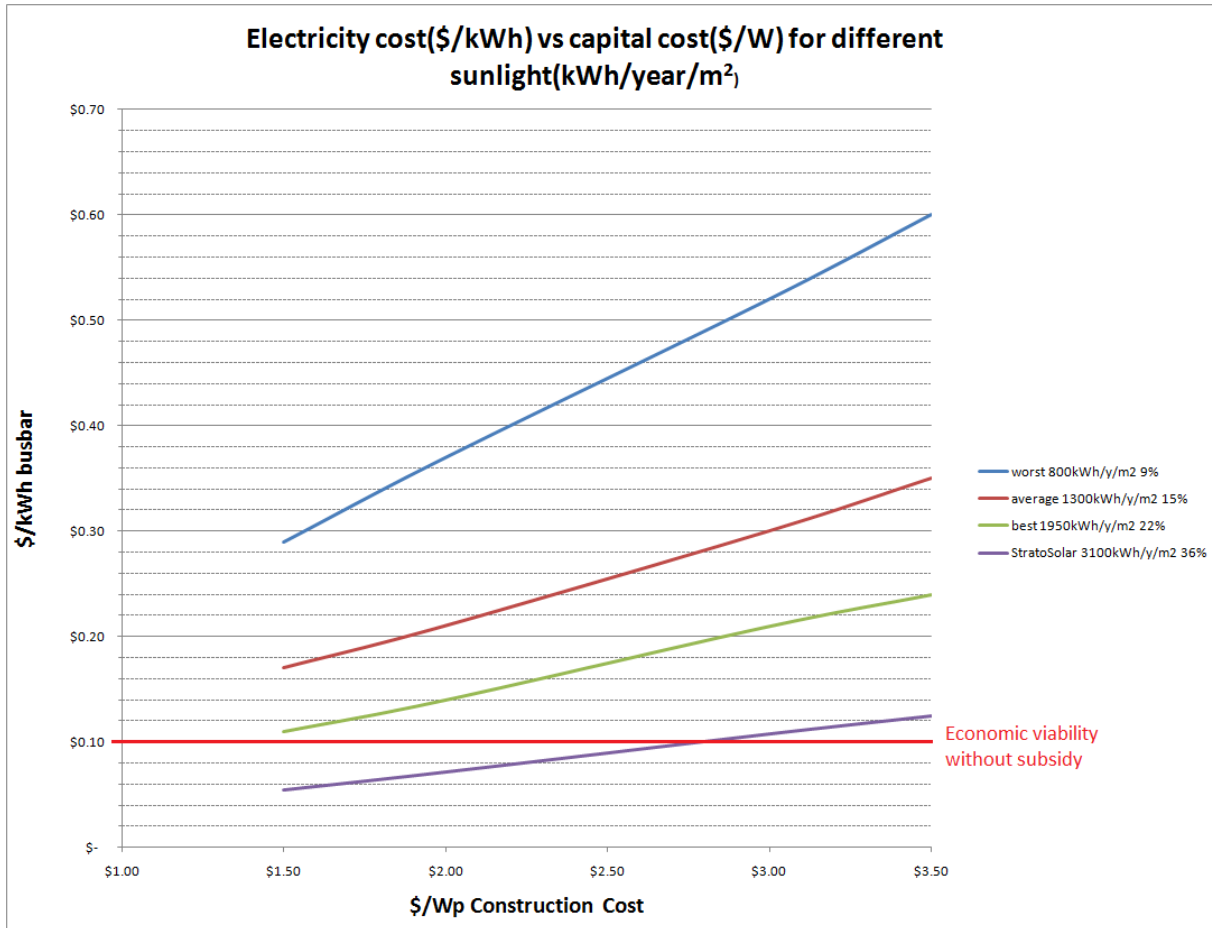


Figure 9 PV electricity cost vs. capital cost for different utilization factors for different locations

July 9, 2011

Figure 9 shows the relationship between capital cost in \$/Wp and the resulting electricity cost in \$/kWh for varying sunlight for different geographic locations. It assumes a 20-year plant life, 8.5% working average cost of capital (WACC) and 2% of capital cost for annual operation and maintenance (O&M).

Worst sunlight is northern Europe, best is US southwest. Sunlight is in average kWh/m²/year. A common way to refer to this variability in power output is to convert it to a utilization or capacity factor percentage. This is useful when comparing different power plants. Using this metric, worst is about 9%, average is about 15%, best is about 22%, and StratoSolar is about a 36% utilization factor.

Given an expected \$/Wp construction cost and a location with known sunlight or its equivalent utilization factor, this chart shows the associated levelized cost of electricity (LCOE) in \$/kWh. Displaying the information in this form graphically illustrates a number of important comparisons while only making assumptions concerning financing.

This chart illustrates several points:

1. The same plant with the same capital cost produces electricity with highly variable cost depending on location. E.g. at the 2010, \$3.50/W capital cost, northern Europe generates electricity for about \$0.60/kWh, and StratoSolar generates electricity for \$0.12/kWh. StratoSolar has the best location (which can be over northern Europe) and lowest cost.
2. The \$3.50/Wp capital cost is approximately the 2010 cost. At historical rates of improvement, the \$1.50/W cost may occur by 2020 at best. Even in the best desert locations, the resulting ground based PV electricity will still cost \$0.12/kWh which will not be competitive without subsidy in 2020.
3. The amount of subsidy required over the next ten years to maintain the historical PV capacity growth rate will become economically difficult to sustain. The historical growth rate would imply 200GWp capacity in 2020 and 1000GWp by 2025.
4. StratoSolar will produce electricity without subsidy with current PV technology \$/Wp capital costs and will benefit equally from the PV \$/Wp improvement path, producing increasingly lower cost electricity.
5. StratoSolar can do this for northern climes.
6. Utility scale PV in the desert needs huge additional investment in electricity distribution and backup generation that is not factored into the PV \$/Wp estimates and also has environmental and political problems.

Cost of Subsidy:

The historical rate of PV plant cost reduction has been approximately 20% for each doubling in capacity manufactured and installed. Figure 10 below shows a projection of this trend forward at current rates until 2027. The future will not unfold as predictably as this graph would imply, but it does give a general sense of the magnitude of things. This rate of improvement from the current cost base will produce a growing and unsustainable subsidy burden as the GWp capacity rises exponentially while the cost of

July 9, 2011

electricity does not fall below \$0.10/kWh until around 2025. If the political will to provide the subsidies that sustain the capacity growth diminishes, then the improvement in the \$/Wp capital costs will slow and the unsubsidized market viability of PV will be delayed beyond 2025. StratoSolar can quickly reduce or eliminate the cost of subsidy and ensure the volume of GWp capacity that will maintain or even increase the rate of cost improvement in PV technology.

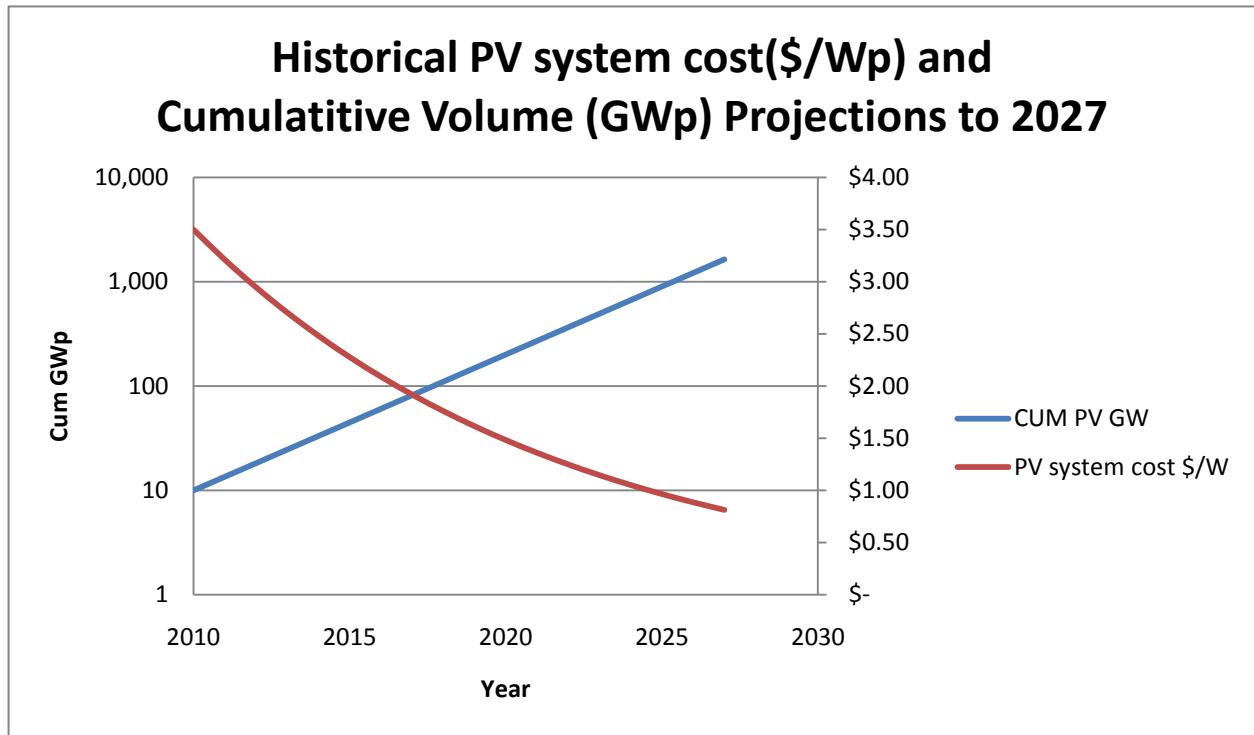


Figure 10 PV system cost and volume projection to 2027

July 9, 2011

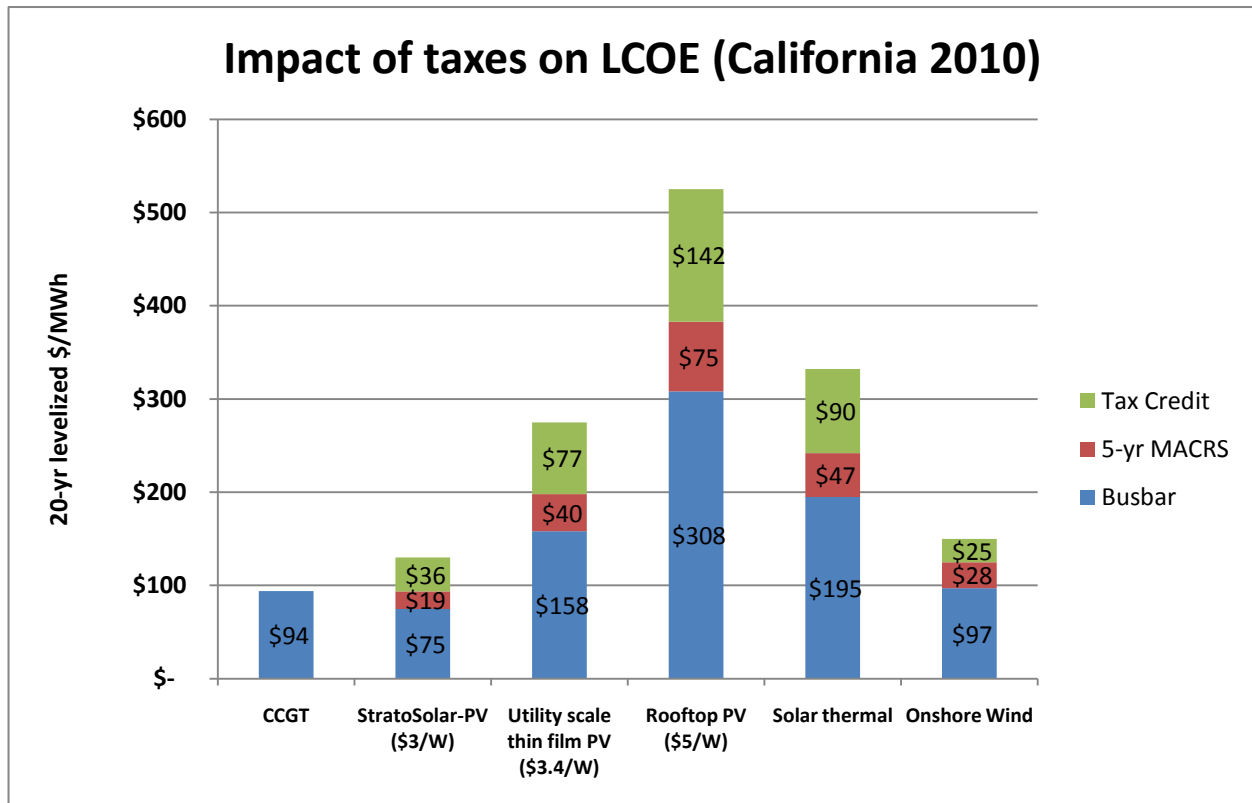


Figure 11 Impact of tax subsidies on levelized cost of electricity

Renewables source: http://www.ethree.com/public_projects/renewable_energy_costing_tool.html.

CCGT source: <http://www.cpuc.ca.gov/PUC/energy/Procurement/LTPP/LTPP2010/2010+LTPP+Tools+and+Spreadsheets.htm>

Figure 11 illustrates the cost of subsidy in California for various energy sources. Busbar shows the \$/MWh cost to utilities. MACRS is accelerated depreciation, and tax credit is effectively a cash rebate. This does not reflect the benefit of loan guarantees or free federal land. Even with all these subsidies, as Figure 11 shows, the California utilities are paying more than market prices for PV electricity.

The CCGT cost in Figure 11 is for combined cycle gas turbine, the dominant power plant type in California. Gas prices have fallen and are predicted to stay low, so the CCGT electricity cost will fall, making PV even less competitive.

July 9, 2011

List of abbreviations:

PV	PhotoVoltaic
DNSI	Direct Normal Solar Insolation
CSP	Concentrated Solar Power
CPC	Compound Parabolic Concentrator
kWh	kilo Watt hours
GWe	Giga Watt electrical
Pa	Pascals
MPa	Mega Pascals
PPA	Power Purchase Agreement
ppm	part per million
PET	PolyEthylene Terephthalate
mrad	milli radian
LEC	Levelized Electricity Cost
O&M	Operation and Maintenance
R&D	Research and Development
WACC	Working Average Cost of Capital
OLF	Optical Light Film
Wh	Watt hours
HAA	High Altitude Airship
UV	Ultra Violet
UHMWPE	Ultra-high-molecular-weight polyethylene
LCOE	Levelized cost of electricity
Wp	Peak Watts, a standard measure of PV panel power output

Bibliography

1. TCOM home page. *TCOM*. [Online] 2010. <http://www.tcomlp.com/aerostats.html>.
2. *POST: A stratospheric telescope for the Antarctic*. **Michael A. Dopita, Holland C. Ford, John Bally, Pierre Bely**. 13, s.l. : Astron. Soc. Aust., 1996, Astron. Soc. Aust., pp. 48-59.
3. **Gregory J. Kolb et al.** *Heliostat Cost Reduction Study*. Albuquerque, NM : Sandia National Laboratories, 2007.
4. **L. M. Murphy, J. V. Anderson, W. Short, T. Wendelin**. *System performance and cost sensitivity comparisons of stretched membrane heliostat reflectors with current generation glass/metal concepts*. Golden, CO : SERI, 1985.

July 9, 2011

5. **Gary Jorgensen et al.** *Advanced reflector materials for solar concentrators*. Golden, Co : NREL, 1995.
6. **A. Palisoc, G. Veal, C. Cassapakis, G. Greschik, M. Mikulas.** *Geometry attained by pressurized membranes*. Tustin, CA : L'Garde, Inc., 1998.
7. **Frederick H. Redell, Justin Kleber, David Lichodziejewski, Dr. Gyula Greschik.** *Inflatable-Rigidizable Solar Concentrators for Space Power Applications*. Tustin, CA : L'Garde Inc., 2004.
8. **E. Onate, B. Kroplin.** *Textile composites and inflatable structures II*. s.l. : Springer, 2008. ISBN 978-1-4020-6855-3.
9. **Roland Winston, Juan C. Minano, Pablo Benitez.** *Nonimaging Optics*. s.l. : Elsevier, 2005. ISBN-13:978-0-12-759751-5.
10. **Imke Durre, Russell S. Vose, David B. Wuertz.** *Overview of the Integrated Global Radiosonde Archive*. Asheville, NC : National Climatic Data Center, 2006.
11. *Enhanced radiosonde data for studies of vertical structure.* **Imke Durre, Xungang Yin.** 2008, BAMS, pp. 1257-1262.
12. **George D. Modica, Thomas Nehrkom, Thomas Myers.** *An investigation of stratospheric winds in support of the high altitude airship*. Lexington, MA : Atmospheric and environmental research Inc., 2006.
13. *Air mass and refraction.* **Young, A. T.** s.l. : Applied Optics. 33:1108–1110, 1991, Vol. 33, pp. 1108–1110.
14. **Tiwari, G.N.** *Solar energy*. s.l. : Alpha science international inc., 2002. ISBN 978-1-84265-106-3.
15. **John A. Duffie, William A. Beckman.** *Solar Engineering of thermal processes*. s.l. : John Wiley and sons, Inc., 2006. ISBN-13 978-0-471-69867-8.
16. **Holms, John D.** *Wind loading of structures*. s.l. : Taylor and Francis, 2001. ISBN10: 0-415-40946-2.
17. **Whitehead, Lorne A.** *Prism Light Guide having surfaces which are in octature*. 4,260,220 USA, 1981. Utility.
18. **Steven G. Saxe, Lorne A. Whitehead, Sanford Cobb, Jr.** *Progress in the development of prism light guides*. St Paul, Mn : 3M Optics technology Center, 1985.
19. *Evaluation of diffraction loss in prism light guides by finite-difference time-domain field modeling.* **Whitehead, Lorne A.** 1998, Applied Optics, p. 5836 to 5842.
20. *Parameterized transmittance model for direct beam and circumsolar spectral irradiance.* **Gueymard, Christian A.** 2001, Solar energy, pp. 325, 346.

July 9, 2011

21. **Ursula Murschall, Ulrich kern, Andreas Stopp, Guenther Crass.** *Transparent, UV resistant, thermoformable film made from crystallizable thermoplastics, and process for its production.* 6,902,818 B2 USA, 2005.
22. *Helium turbomachine design for GT-MHR plant.* **C. F. McDonald, R. J. Orlando, G. M. Cotzas.** Phoenix, AZ : ASME, 1994. International Joint Power generation conference.
23. **Schwartz, Jacob.** *Sensible heat storage unit.* 4,405,010 USA, September 20, 1983. Utility.
24. **James E. Pacheco, Hugh E. Reilly, Gregory J. Colb, Craig E. Tyner.** *Summary of the solar two test and evaluation program.* Albuquerque, NM : Sandia National laboratories, 2000.
25. *High-Temperature Liquid-Fluoride-salt closed-Brayton-cycle solar power towers.* **Charls W. Forsberg, Per F. Peterson, Haihua Zhao.** s.l. : Journal of solar energy engineering, 2007, Vol. 129, pp. 141-146.
26. **Litwin, Robert Z., Hoffman, Nathan J., Zillmer, Andrew J.** *High temperature molten salt solar receiver.* 479635 2006.
27. *Concrete storage for solar thermal power plants and industrial process heat.* **Doerte Laing, Dorothea Lehmann, Carstan Bahl.** 2008. International renewable energy storage conference.
28. **M. P. LaBar, A. S. Shenoy, W. A. Simon, E. M. Campbell.** *The gas-turbine modular helium reactor.* San Diego, CA : General Atomics, 2000.
29. **Per F. Peterson, Charles W. Forsberg, Paul S. Pickard.** *Advanced CSiC composites for high-temperature nuclear heat transport with helium, molten salts, and sulfu-iodine thermochemicalhydrogen process fluids.* s.l. : Argonne National Laboratory, 2002.
30. **D. M. Smith, W. Goodwin, J. A. Schillinger.** *Challanges to the worldwide supply of helium in the next decade.* Allentown, PA : Air Products and Chemicals Inc., 2002.
31. **George A. Olah, Alain Goeppert, G. K. Prakash.** *Beyond oil and gas: the methanol economy.* s.l. : Wiley-VCH, 2006. ISBN-13: 978-3-527-31275-7.
32. **Lovins, Amory B.** *20 Hydrogen myths.* s.l. : Rocky Mountain Institute, 2005.
33. *Desalination: present and future.* **Semiat, Raphael.** s.l. : Water International, 2000, Vol. 25, pp. 54-65.
34. *Thermochemical solar hydrogen generation.* **Licht, Stuart.** s.l. : The royal society of chemistry, 2005, pp. 4635-4646.
35. **Greg Kolb et al.** *Heliostat cost reduction.* s.l. : Sandia National Laboratories, 2007.
36. **Jonathan M. Ross.** *A Practical Approach for Ship Construction Cost Estimating.* s.l. : Proteus Engineering, Anteon Corporation, U.S.A., jross@anteon.com, 2004.

July 9, 2011

Appendix

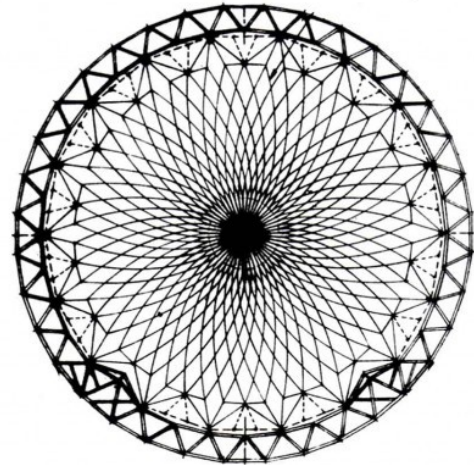
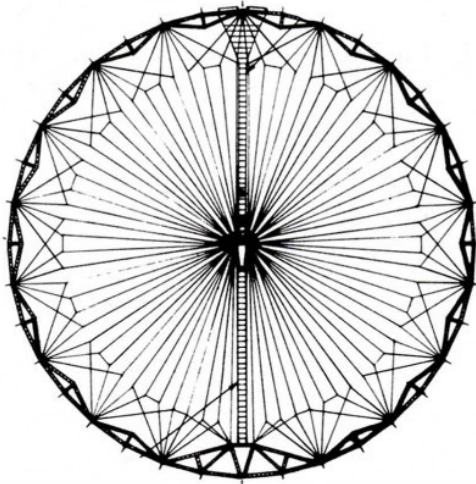
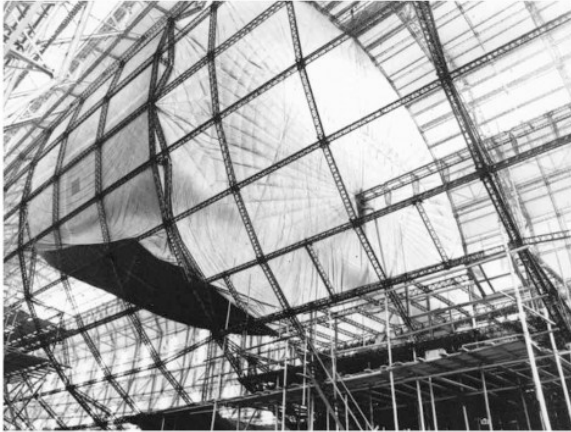


Figure 12 Internal structure of the Hindenburg and the Macon

July 9, 2011



Figure 13 Air force tethered aerostat radar

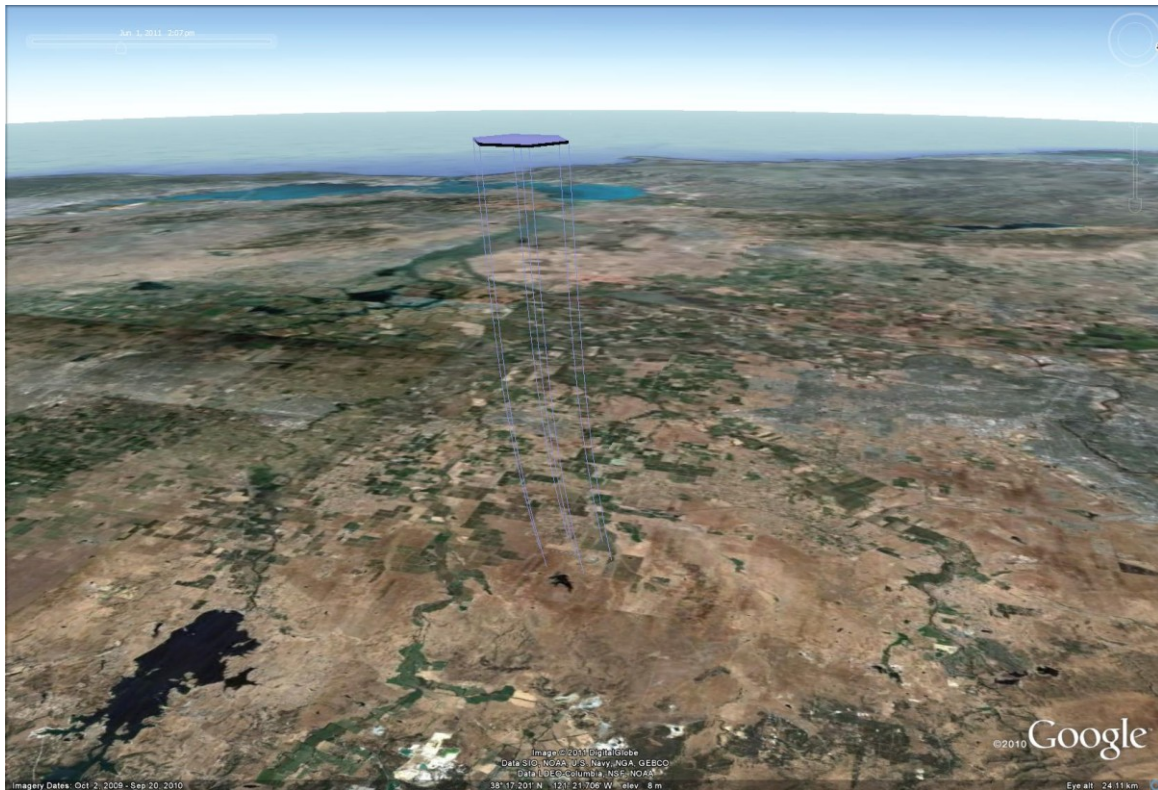


Figure 14 View of a 3,600m PV array from a high-flying aircraft

July 9, 2011

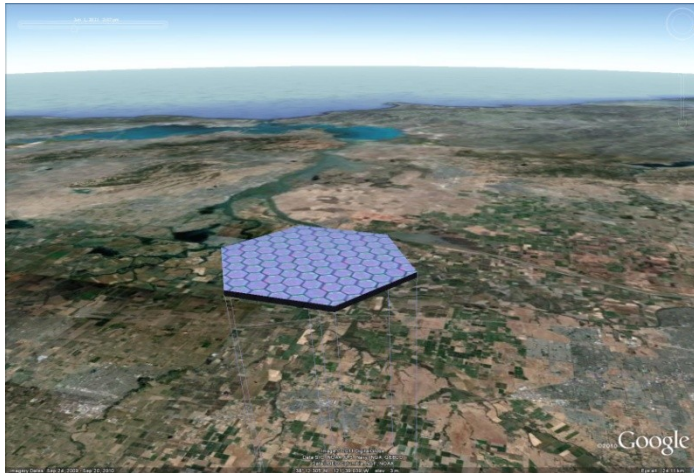


Figure 15 View of a 3,600m PV array from a high-flying aircraft



Figure 16 View of a 3,600m PV array from 10km



Figure 17 View of a 3,600m PV array from 100km

July 9, 2011

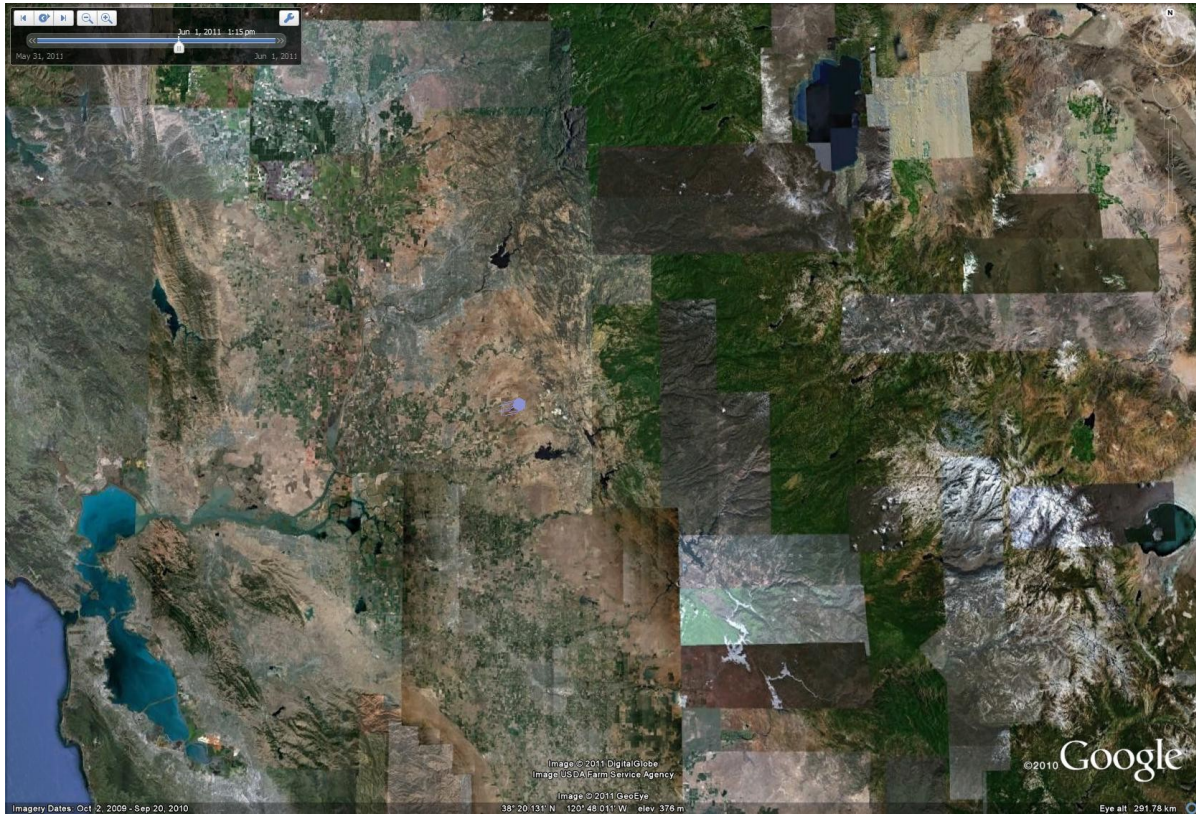


Figure 18 View of a 3,600m PV array from low earth orbit